TEMPORALLY REGULARIZED DIRECT NUMERICAL SIMULATION

WILLIAM J. LAYTON *, C. DAVID PRUETT †, AND LEO G. REBHOLZ ‡

Abstract. Experience with fluid-flow simulation suggests that, in some instances, under-resolved direct numerical simulation (DNS), without a residual-stress model *per se* but with artificial damping of small scales to account for energy lost in the cascade from resolved to unresolved scales, may be as reliable as simulations based on more complex models of turbulence. One efficient and versatile manner to selectively damp under-resolved spatial scales is by a relaxation regularization, e.g. Stolz and Adams [Phys. Fluids (1999)]. We consider the analogous approach based on time scales, time filtering and damping of under-resolved temporal features. The paper explores theoretical and practical aspects of temporally damped fluid flow simulations. We prove existence of unique strong solutions to the resulting continuum model. We also establish the effect of the damping of under-resolved temporal features as the energy balance and dissipation and prove that the time fluctuations $\to 0$ in a precise sense to the temporally damped Navier-Stokes equations. The method is then demonstrated to obtain both steady-state and time-dependent coarse-grid solutions of the Navier-Stokes equations.

Key words. temporal filtering, turbulence, deconvolution, time relaxation

1. Introduction. Direct numerical simulation (DNS) of a $3d$ turbulent flow typically requires $N_{dof}^{NSE} \simeq O(Re^{+9/4})$ mesh points in space per time step, and thus is often not computationally feasible within common time and resource constraints. A promising alternative to DNS is large-eddy simulation (LES). In LES, the evolution of the larger structures in the flow (containing most of the flow's energy) is computed on a relatively coarse grid at reasonable computational expense. The effects of the smaller (unresolved) scales of motion upon the larger ones are modeled. The separation of scales is effected by low-pass filtering in space or time. Filtering the nonlinear terms of the Navier-Stokes equations (NSE) generates subfilter-scale (or residual) stresses, which requires modeling. The approximate deconvolution model (ADM) of Stolz and Adams [SA99] combine a deconvolution model of the residual stress with secondary regularization to stabilize the computation. Recently, Pruett et al. [PTGG06, **?**] have developed a temporal approximate deconvolution model (TADM) based on filtering and defiltering in the time domain rather than in space.

Broadly, an LES model has (at least) tow functions. First, through the model of the filtered nonlinear term, it seeks to model the effect of the unresolved scales on the resolved scales. Second, it mush add sufficient dissipation acting on the marginally resolved scales to remove the energy normally passed from the resolved to unresolved scales by the energy cascade. There has been significant recent work from several directions that suggests that this second function is the more important one and might suffice by itself, for a satisfactory turbulent flow simulation. In particular, we mention the TNS (truncated Navier-Stokes) approach of Domaradzki [Dom05], the VMS (variational multiscale method) of Hughes and co-workers, e.g. [HOM01], and the time relaxation (based on spatial averaging) regularizations of Rosenau [Ros89],

*Department of Mathematics, University of Pittsburgh, PA 15260 (wjl@pitt.edu) Partially supported by NSF grant DMS0810385

†Department of Mathematics, James Madison University, Harrisonburg VA 22807 (pruettcd@jmu.edu)

‡Department of Mathematical Sciences, Clemson University, Clemson SC 29634 (rebholz@clemson.edu) Partially supported by NSF grant DMS0914478

Schochet and Tadmor [ST92], and Stolz, Adams and Kleiser [SAK01a, SAK01b]. This approach is often referred to as "secondary regularization" or "time relaxation."

Given a definition of flow averages, denoted $\overline{u}$, the associated fluctuations are then $u' := u - \overline{u}$. Time relaxation regularization (in its simplest form) consists of adding a term "$+\chi(u - \overline{u})$" to the NSE to damp fluctuations exponentially in time:

$$u_t + u \cdot \nabla u - \nu \Delta u + \nabla p + \chi(u - \overline{u}) = f \text{ and } \nabla \cdot u = 0. \tag{1.1}$$

When u is defined by local spatial averaging, this approach has demonstrated many positive results. It ensures sufficient numerical dissipation for numerical solution of conservation laws [AS02] and does not alter shock speeds or jump conditions, [ELN07]. It can be used quite independently of any turbulence model (and has been so used in compressible flow calculations). As a stand alone regularization, it has been successful for the Euler equations for shock-entropy wave interaction and other tests, [AS02, SAK01a, SAK01b, SAK02], including aerodynamic noise prediction and control (Geunanff [Gue04], see also Åkervik et. al. [ABHHMS06]).

Interestingly, when u is defined by a local and causal time filter, the method has still greater algorithmic attractions and is relatively unexplored. Herein, we investigate some theoretical and practical aspects of this latter approach, called temporally regularized DNS (TRDNS). Time-domain filtering has a number of significant advantages over spatial filtering, Dakhoul and Bedford [DB86] and Pruett [Pru00]. These include

1. There is no filtering through boundaries (and avoidance of the associated problems thereunto, [DJL, DM01]).
2. No difficulties with wall laws (specifying boundary conditions for non-local averages, e.g., [PB02, JLS]).
3. Smooth local transition between DNS, temporal LES, and Reynolds-Averaged Navier-Stokes approaches: $\delta = 0$ corresponds to DNS, $\delta \sim O(\Delta t)$ to TLES and $\delta \to \infty$ to RANS.
4. Ease of cross validation of results with experimental data, which are typically gathered in the time domain.
5. Ease, speed and parallelism in computation. The added work is only one step of an uncoupled ODE (2.1) per mesh point.

Beyond our work herein, all of LES can be redeveloped using temporal filtering. An underlying premise of temporal secondary regularization is that removing energy at high frequencies effectively removes energy at high wavenumbers as well, so that relative to DNS, TRDNS can be conducted at coarser temporal *and* spatial resolution.

Section 2 gives the precise definition of the temporal filter. With $\overline{u}$ defined by (2.1), section 3 gives a theoretical foundation for the system (1.1). We show that the added time relaxation term $\chi(u - \overline{u})$ in (1.1) does truncate scales (Theorem 3.7). We also show that solutions of the NSE are recovered as the filter radius $\to 0$ (Theorem 3.5) and give a precise evaluation of the added energy dissipation. Section 5 gives several tests of both the basic time relaxation term in (1.1), and a higher order version (defined in section 4) and shows their accuracy and great promise for future development.

2. Mathematical Preliminaries. To introduce the time-relaxation term whose effects on the NSE we study herein, we begin with the periodic case. Thus, let $D = (0, L)^3$ and suppose periodic boundary conditions (with the usual zero mean

condition) are imposed,

$$\phi(x + Le_j, t) = \phi(x, t) \text{ and } \int_D \phi(x, t)dx = 0 \text{ for } \phi = u, p, f, u_0.$$

A local temporal filtering operator associated with a time-scale δ must be selected and many are possible. The normal approach is to consider a temporal convolution filter in the theoretical development and then replace this with an approximating initial value problem in practical computations. We shall work directly with an IVP differential filter. For specificity, we choose the temporal differential filter of Pruett et al.[**?**]: given a function $\phi(x, t)$, its time filtered analog $\overline{\phi}$ is the unique solution of

$$\begin{aligned} \frac{d}{dt}\overline{\phi} &= \frac{\phi - \overline{\phi}}{\delta} \text{ , for } t > 0. \\ \overline{\phi}(x, 0) &= \phi(x, 0). \end{aligned} \tag{2.1}$$

This filter is causal, meaning $\overline{\phi}(t)$ depends only on $\overline{\phi}(t')$ and $\phi(t')$ for $t' \leq t$. Further, the application of the filter is "embarrassingly parallel"; its calculation at one mesh point x_i is independent of and uncoupled from its calculation at any other mesh point x_j. Both practical computing and physical intuition indicate that temporal filters in LES should be causal.

3. Theoretical results. Consider the L-periodic (with zero mean) velocity and pressure satisfying

$$\begin{aligned} u_t + u \cdot \nabla u + \nabla p - \nu \triangle u + \chi(u - \overline{u}) &= f, \text{in } D \times (0, T) \\ u(x, 0) &= u_0(x), \text{ in } D \text{ and} \\ \nabla \cdot u &= 0, \text{in } D \times (0, T) \ . \end{aligned} \tag{3.1}$$

The relaxation coefficient χ must be specified and has units $\frac{1}{time}$. We note that the study of (3.1) is additionally relevant to recent work of Åkervik et al. [ABHHMS06] and provides a proof of convergence to a steady-state solution of the NSE for their method.

The analysis of time relaxation involves dimensional analysis coupled with precise mathematical knowledge of (3.1)'s kinetic energy balance. The theory begins, like the Leray theory of the NSE, with a clear global energy balance. It is derived in proposition 3.2, and its proof utilizes the following lemma.

LEMMA 3.1. *For $u \in L^2_0(D \times (0, T))$ and any $T > 0$*

$$\int_0^T \int_D (u - \overline{u}) \cdot u \ dxdt = \frac{\delta}{2}||\overline{u}(T)||^2 - \frac{\delta}{2}||u(0)||^2 + \int_0^T ||u - \overline{u}||^2 dt.$$

Proof. We calculate using $u - \overline{u} = \delta \frac{d}{dt}\overline{u}$ and $u = \overline{u} + \delta \frac{d}{dt}\overline{u}$

$$\begin{aligned} \int_0^T \int_D (u - \overline{u}) \cdot u \ dxdt &= \int_0^T \int_D \delta \frac{d}{dt}\overline{u} \cdot (\overline{u} + \delta \frac{d}{dt}\overline{u}) \ dxdt = \\ &= \frac{\delta}{2}||\overline{u}(T)||^2 - \frac{\delta}{2}||u(0)||^2 + \int_0^T \delta^2 ||\overline{u_t}||^2 dt = \\ &= \frac{\delta}{2}||\overline{u}(T)||^2 - \frac{\delta}{2}||u(0)||^2 + \int_0^T ||u - \overline{u}||^2 dt, \end{aligned}$$

which completes the proof. □

PROPOSITION 3.2. *Let $u_0 \in L^2_0(D), f \in L^2(D\times(0,T))$, and $\int_D f(x,t)dx = 0$. For $\delta > 0$ and $\chi > 0$. If u is a strong solution of (3.1) or a Galerkin approximation in a space of Stokes eigenfunctions, u satisfies for almost every $T > 0$*

$$\frac{1}{L^3}\frac{1}{2}(\|u(T)\|^2 + \chi\delta||\overline{u}(T)||^2) + \int_0^T \frac{1}{L^3}\int_D \nu|\nabla u(t)|^2 + \chi|(u-\overline{u})(t)|^2 dxdt = \frac{1}{L^3}\frac{1}{2}(\|u_0\|^2 + \chi\delta||u_0||^2) + \int_0^T \frac{1}{L^3}\int_D f\cdot u\ dxdt.$$

The above energy bound with equality replaced by "$\leq$" is also satisfied by weak solutions.

Proof. This follows the Navier-Stokes case very closely except for the time relaxation term, e.g., Galdi [Ga00], [Gal95] for a clear and beautiful presentation of the NSE case.

For the energy equality, multiply (3.1) by u, integrate over the domain D, then integrate from 0 to T. This gives

$$\frac{1}{2}\|u(T)\|^2 + \int_0^T\int_D \nu|\nabla u(t)|^2 + \chi(u-\overline{u})\cdot u\ dxdt = \frac{1}{2}\|u_0\|^2 + \int_0^T\int_D f\cdot u\ dxdt. \quad (3.2)$$

From Lemma 3.1 we have

$$\int_0^T\int_D \chi(u-\overline{u})\cdot u dxdt = \chi\left(\frac{\delta}{2}||\overline{u}(T)||^2 - \frac{\delta}{2}||u_0||^2 + \int_0^T ||u-\overline{u}||^2\, dt\right),$$

and the proof is completed by substituting into (3.2). □

REMARK 3.3. *By the above lemma and energy estimate, the model's relaxation term thus extracts energy from resolved scales. Thus, we can define an energy dissipation rate induced by time relaxation for (3.1) as*

$$\varepsilon_{\ model}(u)(t) := \frac{1}{L^3}\int_D \nu|\nabla u(t)|^2 + \chi|(u-\overline{u})(t)|^2 dx \quad (3.3)$$

The models kinetic energy is

$$E_{\ model}(u)(t) := \frac{1}{L^3}\frac{1}{2}(\|u(t)\|^2 + \chi\delta||\overline{u}(t)||^2) \quad (3.4)$$

The following analytic estimate of the effect of the relaxation term follows easily from the above energy estimate.

COROLLARY 3.4. *There exists a weak solution to (3.1) satisfying*

$$||u||^2_{L^\infty(0,T;L^2(D))} + ||\nabla u||^2_{L^2(0,T;L^2(D))} \leq C(\nu, f, u_0, \chi, \delta),$$
$$||\overline{u}||^2_{L^\infty(0,T;L^2(D))} + ||\overline{u}_t||^2_{L^2(0,T;L^2(D))} + ||u-\overline{u}||^2_{L^2(0,T;L^2(D))} \leq C(\nu, f, u_0, \chi, \delta).$$

Moreover, if a weak solution u is a strong solution, then it is also unique.

Proof. This follows the NSE case closely. Equation 3.1 is a linear, zeroth order perturbation of the NSE and its solution satisfies a stronger á priori estimate than

the NSE case. Thus the standard existence proof of Galerkin approximation, á priori estimation and extracting a limit as the number of Galerkin modes increases works here exactly as in the NSE case, e.g. Galdi [Gal95]. □

THEOREM 3.5. *Let $u(x,t;\chi,\delta)$ denote a weak solution of (3.1) and let $u_{NSE}(x,t)$ denote a weak solution of the NSE (i.e., (3.1) with $\chi = 0$). As $\delta \to 0$ there is a subsequence $\delta_j \to 0$ and a weak solution of the NSE such that such that $u(x,t;\chi,\delta_j) \to u_{NSE}(x,t)$ as $\delta_j \to 0$. If u_{NSE} is a strong solution then $u(x,t;\chi,\delta) \to u_{NSE}(x,t)$ in $L^2(0,T;L^2(\Omega))$ as $\delta \to 0$.*

Proof. This follows the proof in the case of spatial filtering e.g. [LN06]. □

PROPOSITION 3.6. *Let u be a weak solution of (3.1), $u_0 \in H^1(D)$, $\delta > 0$, and $\chi > 0$, then*

$$ess - \sup_{[0,T]} ||\nabla \overline{u}|| \leq C(\delta, \nu, f, u_0) < \infty.$$

Proof. Since

$$\overline{u}_t = \frac{u - \overline{u}}{\delta}, (\nabla \overline{u})_t = \frac{\nabla u - \nabla \overline{u}}{\delta}.$$

Thus, for any $T \geq 0$

$$\nabla \overline{u}(T) = e^{-\frac{1}{\delta}T} \nabla u_0 + \int_0^T e^{-\frac{1}{\delta}(T-t)} \nabla u(t) dt.$$

Taking norms of both sides and applying the generalized triangle and Cauchy-Schwarz inequalities gives

$$||\nabla \overline{u}(T)|| \leq C(data) + T^{\frac{1}{2}} \int_0^T ||\nabla u(t)||^2 dt \leq C(data).$$

□

The limit as the averaging radius $\delta \to 0$ is technically intricate but follows closely early work of J. Leray (and elaborations of this work). The other limiting case is equally important and nontrivial. Since the purpose of the time relaxation term is to drive fluctuations to zero, as χ increases the fluctuating part of u should go to zero if the term is performing as intended. The next theorem shows that this is indeed true, and the key to its proof is the next estimate.

THEOREM 3.7. *Let u be a weak solution of (3.1). If $\nabla u_0 \in L^2(D)$, $\delta > 0$ and $f \in L^2(0,T;L^2(D))$ then there is a $C = C(u_0, f, T)$ such that as $\chi \to \infty$*

$$\int_{D\times(0,T)} |u(x,t) - \overline{u}(x,t)|^2 dx dt \to 0, \tag{3.5}$$

$$\int_{D\times(0,T)} |\overline{u}_t(x,t)|^2 dx dt \to 0 \ . \tag{3.6}$$

and thus $u' \to 0$ in $L^2(D \times (0,T))$ as $\chi \to \infty$.

Proof. Begin with the energy estimate for weak solutions

$$\frac{1}{L^3}\frac{1}{2}(\|u(T)\|^2+\chi\delta||\overline{u}(T)||^2)+\int_0^T\frac{1}{L^3}\int_D\frac{\nu}{2}|\nabla u(t)|^2+\chi|(u-\overline{u})(t)|^2dxdt\leq$$
$$\frac{1}{L^3}\frac{1}{2}(\|u_0\|^2+\chi\delta||u_0||^2)+\int_0^T\frac{1}{2\nu L^3}||f||_*^2dt.$$

Divide by χ and let $\chi\to\infty$. This gives

$$\frac{\delta}{2}||\overline{u}(T)||^2+\int_0^T\int_D\chi|(u-\overline{u})(t)|^2dxdt-\frac{\delta}{2}||u_0||^2\to 0. \tag{3.7}$$

Next, take the inner product of the model (3.1) with $u-\overline{u}$. This gives (since $\nabla\cdot(u-\overline{u})=0$)

$$\int_0^T[\frac{1}{2}\frac{d}{dt}||u||^2-(u_t,\overline{u})-(u\cdot\nabla u,\overline{u})+\chi||u-\overline{u}||^2-(f,u-\overline{u})]dt=0. \tag{3.8}$$

For the first two terms, we use the filter equation and Corollary 3.4 to find

$$\begin{aligned}&\int_0^T[\frac{1}{2}\frac{d}{dt}||u||^2-(u_t,\overline{u})]dt\\&=\int_0^T[\frac{1}{2}\frac{d}{dt}||u||^2-\frac{d}{dt}(u,\overline{u})-(u,\overline{u}_t)]dt\\&=\int_0^T\frac{d}{dt}[\frac{1}{2}||u||^2-(u,\overline{u})]+\frac{1}{\delta}(u,u-\overline{u})]dt\\&\leq C(data).\end{aligned}$$

For the forcing term we employ a similar argument. The nonlinear term requires a bit more care. By the standard bound for the nonlinear term:

$$\int_0^T(u\cdot\nabla u,\overline{u})dt\leq C\int_0^T||\nabla u||^2||\nabla\overline{u}||dt$$
$$\leq C(ess-\sup_{[0,T]}||\nabla\overline{u}||)\int_0^T||\nabla u||^2dt\leq C(data),$$

by the regularity result of Proposition 3.6.

Thus we have

$$\int_0^T\chi||u-\overline{u}||^2dt\leq C(data).$$

Thus as $\chi\to\infty$, $\int_0^T||u-\overline{u}||^2dt\to 0$, as claimed. □

4. Secondary regularization with temporal deconvolution. We now consider the process of temporal deconvolution (defiltering). The ill-posed deconvolution problem is central in image processing [BB98] and residual-stress modeling in spatially averaged large eddy simulation [BIL06], [Gue97], [LL03], [LL04c], [LL05]. The basic problem in approximate deconvolution is the following: given $\overline{u}$ find *useful* approximations of u. In other words, solve the following equation for an approximation which is appropriate for the application at hand:

$$Gu=\overline{u},\ \text{solve for } u.$$

TABLE 4.1
Coefficients d_k for secondary deconvolution of selected degrees N.

	$N=4$	$N=3$	$N=2$	$N=1$	$N=0$
d_0	2 + 59/128	35/16	15/8	3/2	1
d_1	-2 - 69/128	-29/16	-9/8	-1/2	NA
d_2	1 + 62/128	12/16	2/8	NA	NA
d_3	- 60/128	-2/16	NA	NA	NA
d_4	+ 8/128	NA	NA	NA	NA

The original spatial-deconvolution method used by Stolz, Adams and Kleiser [SAK01a] was the van Cittert algorithm. Unfortunately, previous work in [PTGG06] has shown the van Cittert deconvolution to be *unstable* for the temporal filter of (2.1) and most likely for any causal time filter. However, a stable linear deconvolution algorithm was developed expressly for the differential filter of (2.1) by Pruett et. al. [PTGG06]. It is defined by

$$\phi \approx D_N\overline{\phi} \equiv \sum_{k=0}^{N} d_k \overline{\phi}^{(k+1)}. \tag{4.1}$$

where N denotes the *degree* of the deconvolution, $\overline{\phi}^{(k)}$ denotes a k-time temporally filtered field, and coefficients d_k are given in table 4.1 for the first few degrees. In addition to stability, these coefficients are designed to recover low frequency content lost through the filter while attenuating high frequency content. For their derivation, e.g. if higher order coefficients are desired, we refer the reader to [PTGG06, Pru08]. This leads to the model with secondary deconvolution regularization

$$\begin{aligned} u_t + u\cdot\nabla u + \nabla p - \nu\triangle u + \chi(u - D_N\overline{u}) &= f, \text{in } D\times(0,T) \\ u(x,0) &= u_0(x), \text{ in } D \text{ and} \\ \nabla\cdot u &= 0, \text{in } D\times(0,T). \end{aligned} \tag{4.2}$$

Temporal deconvolution methods are just beginning to be studied and their theory is not as clear as the zeroth order deconvolution case (i.e. $N = 0$) studied in section 3. Thus we leave the extension of the theory to $N > 0$ as an interesting open problem. However, we were able to extend the methodology to the $N > 0$ case; in section 5 we give comparisons of $N = 0$ and $N = 4$ deconvolution within secondary regularization.

5. Numerical Results. In this section, the theoretical results of the previous sections are corroborated by three computational demonstrations of TRDNS: 1) the stabilization of an unstable, two-dimensional free-shear flow, 2) determination of a steady-state solution for a highly unstable two-dimensional boundary-layer flow, and 3) selective frequency damping in a three-dimensional highly unstable boundary-layer flow.

5.1. Stabilization of Free-Shear Flow. Free-shear flows result when two adjacent fluid streams travel at differing velocities. The internal boundary layer generated at the interface is inviscidly unstable to small perturbations. As a result the interface is subject to Kelvin-Helmholtz instability, which is characterized by rapid growth of disturbances and the shedding of a von Karman vortex street. The discrete vortices of the vortex street are typically separated by a distance of one wavelength

of the most unstable frequency. If a subharmonic frequency is also present, adjacent vortices experience downstream pairing.

Figure 5.1 shows a snapshot in time in the spatial evolution of a two-dimensional mixing layer. The flow is from left to right. The velocity ratio of the upper stream to the lower one is 0.181. This particular case was studied in 1989 by Pruett [Pru89]. Fluid parameter values, non-dimensionalization, and computational parameter values can all be found in this paper, as can details of the numerical scheme.

Briefly, regarding the latter, the two-dimensional incompressible NSE are solved in an $\omega - \psi$ formulation, ω being vorticity and ψ being streamfunction. The governing system is thereby comprised of a transport equation for vorticity and a Poisson equation for the streamfunction. The highly efficient semi-explicit numerical scheme of Kim and Moin [KM85] is exploited, which blends approximate factorization of linear (diffusion) terms with explicit second-order Adams-Bashforth treatment of nonlinear (advection) terms of the transport equation. The Poisson equation for streamfunction is solved by a fast-elliptic solver that exploits Fourier techniques. Centered differences are used for spatial derivatives rendering the algorithm of second-order accuracy in time and space.

The mixing-layer flow of interest is forced at the inflow (left) boundary at a frequency very close to its most unstable frequency, as determined by solution of the Rayleigh equation. (See Fig. 4 of [Pru89].) The forcing amplitude of the fundamental ($A_1 = 0.001$) is quite low. A weak subarmonic of amplitude $A_{1/2} = 0.0001$ is also included. Figure 5.1 results from a simulation of undamped flow; that is, with no temporal regularization. The von Karman vortex street and incipient vortex pairing are readily apparent. The streamwise (x) and transverse coordinates (y) in the figure are scaled by momentum thickness θ and U_T/β, respectively, where U_T is the velocity of the upper stream and β is the circular frequency of the imposed disturbance. The two most fundamental parameters of the flow are the Reynolds number $Re = U_t^2/(\nu\beta) = 185.6$, where ν is kinematic viscosity, and the Strouhal number $Str = \beta\theta/U_T = 0.114$, which characterizes the fundamental forcing frequency.

Figure 5.2 portrays the same forced mixing layer subject to artificial stabilization via low-degree ($N = 0$) secondary regularization. The physical time of the snapshot is that same as that of Fig. 5.1, and flow parameters for Fig. 5.2 are identical to those of Fig. 5.1. However, a regularization term of the form of that in Eq. (1.1) has been appended to the vorticity transport equation. Specifically, the regularization term is $\chi(\omega - \bar{\omega})$, where $\bar{\omega}$ is evolved in time along with the solution via an equation analogous to Eq. (2.1). The damping parameters are $r = \delta/T = 0.5$ and $\chi = 0.5$, where T is the period of the fundamental. It is interesting to note that the most unstable frequency is completely stabilized. Moreover, for this flow, all frequencies within the wide band $0 \leq Str \leq 0.37$ are unstable, as shown in Fig. 4 of [Pru89]. Apparently, all unstable modes are stabilized by the regularization term. Recall that the main result of this paper concludes that, for a fixed $\delta > 0$, disturbances of all frequencies can be stabilized for "sufficiently large" χ. Present results showing the complete stabilization of a highly unstable forced mixing layer by temporal secondary regularization corroborate our theoretical result and reveal that "sufficiently large" in theory is relatively small in practice.

5.2. Laminar Base States of Unstable Flows. Until quite recently, numerical experiments of spatially transitioning flows had a problematic Achilles heel. Such flows transition from laminar to turbulent states because they are unstable to certain perturbations. Thus, in numerical transition experiments, one, by definition, inves-

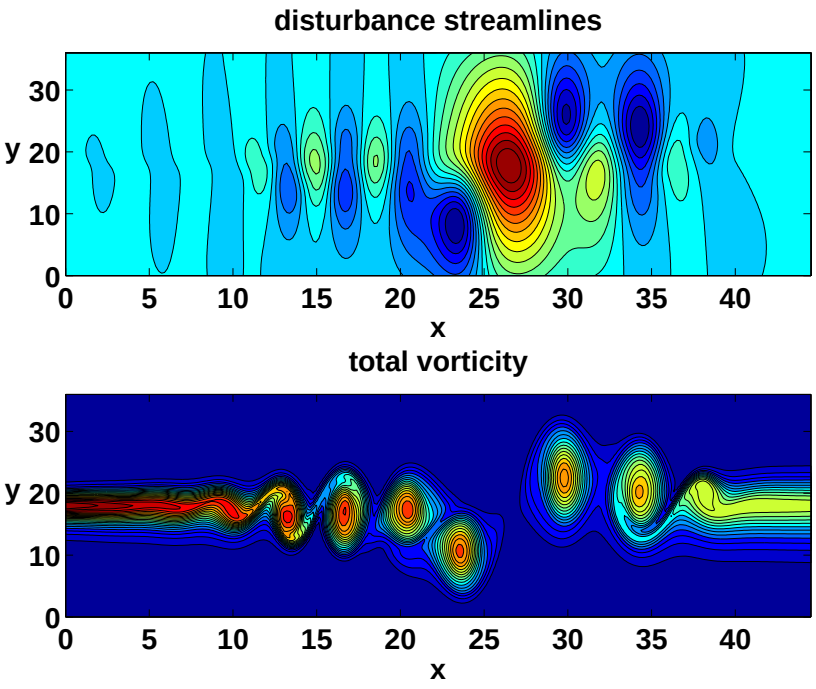

FIG. 5.1. *Contours of disturbance streamfunction and total vorticity and in undamped planar mixing layer at time equivalent to eight periods of forcing at most unstable frequency. The flow, left to right, demonstrates Kelvin-Helmholtz instability characteristic of mixing layers. Contour levels of disturbance streamfunction range in equal increments between -0.2753 and +0.5492; contours of total vorticity range from -0.004 to 0.1914.*

tigates the hydrodynamic stability of perturbed laminar and time-independent base states. However, the very instability of the base state makes the numerical determination of such a state extremely difficult for high-order, non-dissipative numerical methods, because numerical noise triggers the instabilities. In short, there was until recently no universally satisfactory method for obtaining high-order time-independent solutions of the NSE in the case of unstable flows.

In 2006 Åkervik et al. [ABHHMS06] adapted temporal secondary regularization of Pruett et al. [**?**, PTGG06] to the computation of time-independent solutions of globally unstable flows by relaxation methodology. Essentially their methodology exploits low-order temporal secondary regularization ($N = 0$), with χ sufficiently large to dampen all unstable frequencies, including the fundamental, so that a time-dependent calculation relaxes toward a steady state. Theorem 3.7 undergirds their work by essentially stating that such a χ always exists.

To demonstrate the utility of secondary regularization, we consider the test case that one of Åkervik's collaborators (Marxen) considered for his Ph.D. dissertation. Specifically, we consider flat-plate boundary-layer flow subject to an adverse pressure gradient. In such scenarios, the relatively weak viscous Tollmien-Schlicting instability of boundary-layer flow is destabilized by adverse pressure gradient leading to rapid transition from laminar to turbulent flow. As a consequence the base state of such a flow is virtually impossible to compute without artificial stabilization.

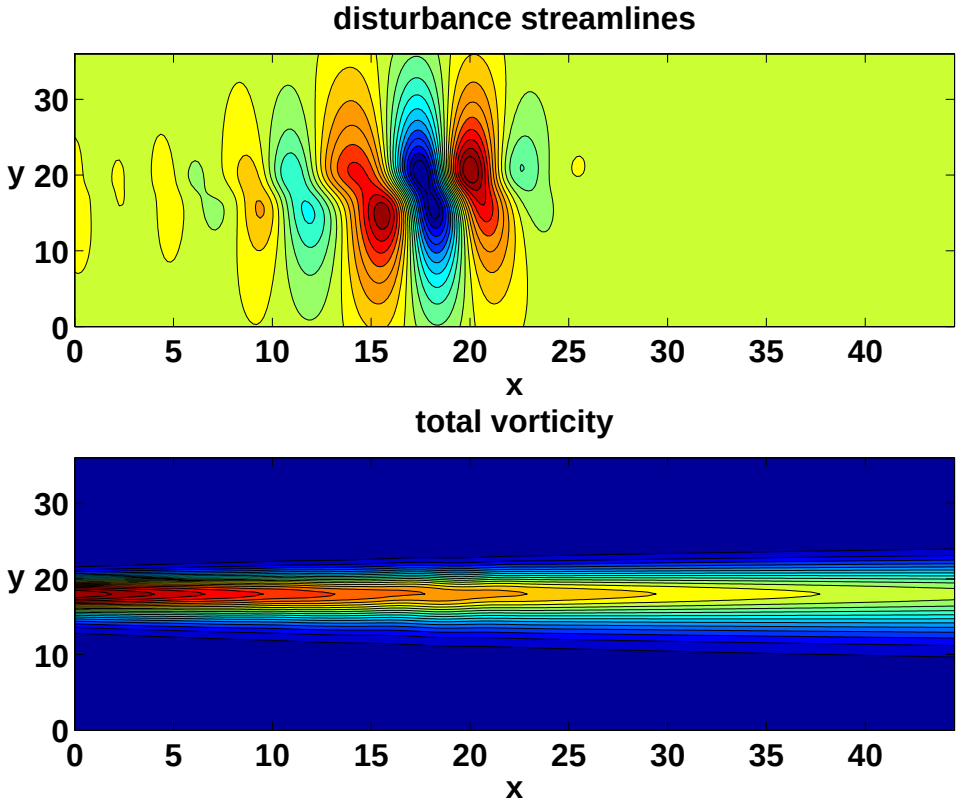

FIG. 5.2. *Contours of disturbance streamfunction and total vorticity and in a temporally damped planar mixing layer at time equivalent to eight periods of forcing at most unstable frequency. Contour levels of disturbance streamfunction range in equal increments between -8.715* $\times 10^{-4}$ *and +7.129* $\times 10^{-4}$*; contours of total vorticity range from 0.0 to 0.1914.*

The parameter values of the test case and the numerical methodology can be found in Marxen [Marx04]. Briefly, the high-order numerical methodology combines fourth-order and sixth-order compact finite-difference techniques for streamwise and wall-normal discretizations, respectively with Fourier pseudospectral methods (with dealiasing) for the spanwise discretization and the classic fourth-order Runge-Kutta method for time integration. Marxen's DNS results were computed with spatial resolution in the streamwise x and wall-normal y dimensions of 1970 and 225 grid points, respectively, with 64 symmetric Fourier modes in the spanwise z dimension, and with 1600 steps in time for each fundamental period of the disturbance.

The flow, at $Re_{\delta_1} = 580$, the Reynolds number based on boundary-layer displacement thickness δ_1 at the inflow boundary, is forced by a disturbance strip along the wall just downstream of the leading edge and activated by low-level periodic suction and blowing at fundamental frequency β_0. In a boundary layer without pressure gradient, the disturbance strip generates Tollmien-Schlicting waves that initially grow relatively slowly according to linear stability theory. The effect of adverse pressure gradient downstream of the disturbance strip, however, is to induce a separation bubble that greatly destabilizes the flow. The resulting instabilities are explosive in nature, and the flow transitions from laminar to turbulent within a very few wave-

lengths downstream of the disturbance strip.

Here, we demonstrate the ability of heavily damped TRDNS to obtain a steady solution of the NSE for the highly unstable separation bubble problem. The unsteady, NSE are solved in a vorticity-velocity formulation and in disturbance form. Accordingly, the regularization term is added to the right-hand side of the vorticity transport equations. The spatial resolution of the computation is 978 x 113, with 4 Fourier modes in the spanwise dimension, and the resolution in time is 600 steps per fundamental period.

When the differential filtered of (2.1) is implemented via a discrete time-evolution scheme, in this case fourth-order Runge-Kutta, it is natural to parameterize the filter width δ as a fraction of some characteristic time scale, in this case the period of the fundamental.

The regularization parameters are as follows. As stated previously, $N = 0$. The damping coefficient χ is large, namely $\chi = 4.0$. And $r = 0.5\tau_0$, where $\tau_0 = 2\pi/\beta_0$ is the fundamental forcing period. That is, the temporal filter width is 50 percent of the period of the fundamental of the most unstable frequency. For base-state computations, the forcing is turned off by setting the forcing amplitude to zero.

The initial state is, of course, not an exact solution of the discretized time-independent NSE, namely because determining such an illusive state is the goal of the computation. As a result, the initial state, typically derived from the boundary-layer equations, represents a small perturbation of an exact solution. On interest is how the initial solution evolves toward the exact two-dimensional, steady-state solution.

To this end, Fig. 5.3 tracks the evolution of the spanwise component of disturbance vorticity θ_3 as a function of time. The figure presents extrema of disturbance vorticity and their streamwise locations as functions of time. The figure suggests that there is a transient sweep event in which the initial error propagates downstream like a wave packet subject to extreme damping. The transient growth of the extrema over some short time intervals is most likely due to constructive interference of damped traveling waves at differing frequencies. Following the exit of the wavefront from the computational domain, the disturbance vorticity decays exponentially in time. Thus, with regularization parameters that impose heavy damping, the regularized NSE are stable to perturbations at all frequencies, apparently including three-dimensional ones. At steady state, the regularization term vanishes, and thus, a time-independent solution of the NSE can be attained after sufficiently long integration.

5.3. Temporally Regularized DNS. Our final result represents a computational extrapolation beyond the theoretical scope of this paper.

Higher degree ($N > 1$) temporal regularization has been shown to evoke selective freqency damping [PGGT03, Pru08], which suggests that TRDNS could be an attractive alternative to LES. Although our main theoretical result applies only to $N = 0$ regularization, we nevertheless demonstrate the utility of high-order TRDNS methodology for selective frequency damping.

Once again, we consider the test case of Marxen [Marx04]: flow along a flat plate subject to adverse pressure gradient.

We repeat the previous calculation with $N = 4$, $\chi = 2.5$, and $r = 0.4$, parameter values designed to permit low-frequency disturbances to evolve more-or-less naturally, but to provide extreme dissipation to high-frequency traveling waves. The resolution parameters are the same as before, except that the number of spanwise modes is increased dramatically to 32 to accommodate three-dimensional instabilities characteristic of transitional flow. At this resolution, the coarse-grid TRDNS represents a

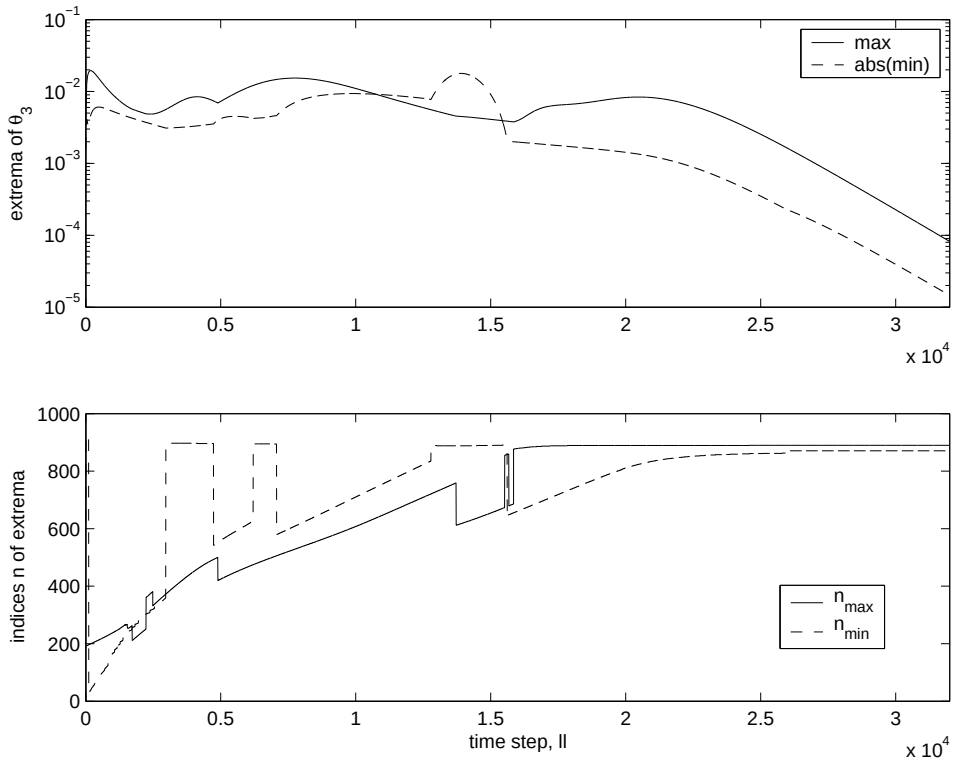

FIG. 5.3. *Time evolution of extrema of spanwise component of disturbance vorticity for over-damped $N = 0$ TRDNS showing convergence in time toward a time-independent solution of the NSE.*

reduction in computational effort relative to the DNS of Marxen by a factor of roughly 20. For this case, the forcing amplitude is non-zero but small, namely 10^{-4}, with a slight spanwise variation.

Figure 5.4 presents the same information as Fig. 5.3 for the forced TRDNS case. There is an initial transient period of rapid growth of the vorticity maximum, a subsequent period of roughly exponential growth, a third transitional period, and a final period of apparently stationary "turbulent" flow characterized by vorticity fluctuations that are a sizeable percentage of the mean vorticity.

Based upon the experience of Marxen [Marx04] and the second author's experience with the same code, without regularization, a simulation at this resolution is severely under-resolved and blows up as soon as the instabilities attain appreciable amplitudes.

6. Discussion and Conclusions. Time relaxation regularization is a promising yet understudied method of truncating scales for under-resolved flow simulation. Because the additional computational effort stems from solving linear ODEs, the computational overhead of temporal regularization is relatively small. Moreover, the methodology is readily parallelizable. Experience to date with TRDNS suggests that it has a variety of useful applications and is worthy of further investigation.

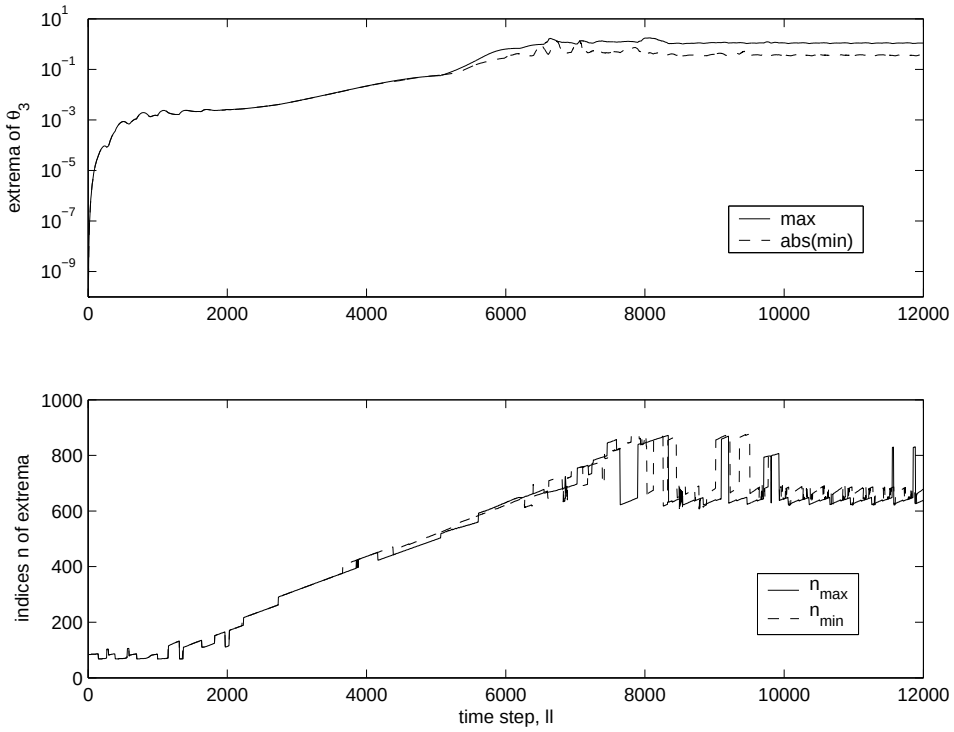

FIG. 5.4. *Time evolution of extrema of spanwise component of disturbance vorticity for forced TRDNS with* $N = 4$, $\chi = 2.5$, *and* $r = 0.4$.

ACKNOWLEDGEMENT 6.1. *The authors are grateful to the Institute for Aerodynamics and Gasdynamics at the University of Stuttgart for access both to their computing cluster and computational code for boundary-layer flow. Special thanks is due Olaf Marxen for tirelessly assisting the second author in compiling, executing, and understanding that code.*

REFERENCES

[AS01] N. A. ADAMS AND S. STOLZ, *Deconvolution methods for subgrid-scale approximation in large eddy simulation*, Modern Simulation Strategies for Turbulent Flow, R.T. Edwards, 2001.

[AS02] N. A. ADAMS AND S. STOLZ, *A subgrid-scale deconvolution approach for shock capturing*, J.C.P., 178 (2002),391-426.

[ABHHMS06] E. ÅKERVIK, L. BRANDT, D. S. HENNINGSON, J. HŒPFFNER, O. MARXEN, P. SCHLATTER, *Steady solutions of the Navier-Stokes equations by selective frequency damping*, Phys. Fluids, 18, (2006), 068102.

[BB98] M. BERTERO AND B. BOCCACCI, *Introduction to Inverse Problems in Imaging*, IOP Publishing Ltd.,1998.

[BIL06] L. C. BERSELLI, T. ILIESCU AND W. LAYTON, *Mathematics of Large Eddy Simulation of Turbulent Flows*, Springer, Berlin, 2006.

[DB86] Y. M. DAKHOUL AND K. W. BEDFORD, *Improved averaging method for turbulent flow simulation. Part I: Theoretical development and application to Burger's transport equation*, Int. J. Numer. Methods Fluids, 6 (1986), p. 49.

[DM01] A. DAS AND R. MOSER, *Filtering boundary conditions for LES and embedded boundary simulations* in: C. Liu, L. Sakell, and T. Beutner, editors, *DNS/LES progress and challenges*, pages 389-396, Columbus, 2001. Greyden Press.

[Dom05] J. A. DOMARADZKI, *Modeling challenges and approaches in LES for physically complex*

flows in: Large-Eddy Simulation of Complex Flows, proceedings of Euromech Colloquium 469, Technical University Dresden, Germany, Oct. 6-8, 2005, p. 84.

[DE06] A. Dunca and Y. Epshteyn, *On the Stolz-Adams de-convolution LES model*, SIAM J. Math. Anal. 37 (6), (2006), 1890-1902.

[DJL] A. Dunca, V. John and W. Layton, *The Commutation Error of the Space Averaged Navier-Stokes Equations on a Bounded Domain*, in: Contributions to current chal lenges in mathematical uid mechanics, 5378, Adv. Math. Fluid Mech. Birkhauser, Basel, 2004.

[ELN07] V. J. Ervin, W. J. Layton and M. Neda, *Numerical analysis of a higher order time relaxation model of fluids*, International Journal of Numerical Analysis and Modeling, 4, (2007) 648-670.

[F97] C. Foias, *What do the Navier-Stokes equations tell us about turbulence?* Contemporary Mathematics, 208(1997), 151-180.

[FHT01] C. Foias, D. D. Holm and E. Titi, *The Navier-Stokes-alpha model of fluid turbulence*, Physica D, 152-153(2001), 505-519.

[Fr95] U. Frisch, *Turbulence*, Cambridge, 1995.

[Ga00] G. P. Galdi, *Lectures in Mathematical Fluid Dynamics*, Birkhauser-Verlag,2000.

[Gal95] G.P. Galdi, *An introduction to the Mathematical Theory of the Navier-Stokes equations, Volume I*, Springer, Berlin, 1994.

[GL00] G. P. Galdi and W. J. Layton, *Approximation of the large eddies in fluid motion II: A model for space-filtered flow*, Math. Models and Methods in the Appl. Sciences, 10(2000), 343-350.

[GE86] M. Germano, *Differential filters of elliptic type*, Phys. Fluids, 29(1986), 1757-1758.

[Gue97] B. J. Geurts, *Inverse modeling for large eddy simulation*, Phys. Fluids, 9(1997), 3585.

[Gue04] R. Guenanff, *Non-stationary coupling of Navier-Stokes/Euler for the generation and radiation of aerodynamic noises*, PhD thesis: Dept. of Mathematics, Universite Rennes 1, Rennes, France, 2004.

[HOM01] T. J. R. Hughes, A. A. Oberai and L. Mazzei, *Large Eddy Simulation of Turbulent Channel Flow by the Variational Multiscale Method*, Phys. Fluids, 13 (2001) 1784-1799.

[Volk04] V. John, *Large Eddy Simulation of Turbulent Incompressible Flows,* Springer, Berlin, 2004.

[KM85] J. Kim and P. Moin, *Application of a fractional-step method metod to the incompressible Navier-Stokes equations*, J. Comput. Phys., 59 (1985), 308-323.

[JLS] V. John, W. Layton, and N. Sahin, *Derivation and Analysis of Near Wall Models for Channel and Recirculating Flows*, Comput. Math. Appl. 48 (2004), 1135 - 1151.

[Lad69] O. Ladyzhenskaya, *The Mathematical Theory of Viscous Incompressible Flow*, Gordon and Breach, 1969.

[LL03] W. Layton and R. Lewandowski, *A simple and stable scale similarity model for large eddy simulation: energy balance and existence of weak solutions*, Applied Math. Letters 16(2003) 1205-1209.

[LL05] W. Layton and R Lewandowski, *On a well posed turbulence model*, Discrete Contin. Dyn. Syst. Ser. B 6 (2006), 111128.

[LL04c] W. Layton and R Lewandowski, *Consistency and feasibility of approximate deconvolution models of turbulence*, Tech. Report, Dept. of Mathematics, Univ. of Pittsburgh, 2005.

[LN06] W. Layton and M. Neda, *Truncation of scales by time relaxation*, Journal of Mathematical Analysis and Applications 325 (2007), 788-807

[Les97] M. Lesieur, *Turbulence in Fluids*, Kluwer Academic Publishers, 1997.

[MK05] C. Manica and S. Kaya, *Convergence analysis of the finite element method for a fundamental model in turbulence*, Tech. Report, Dept. of Mathematics, Univ. of Pittsburgh, 2005.

[Marx04] O. Marxen, *Numerical studies of physical effects related to the controlled transition process in laminar separation bubbles*, Dissertation for Doctorate of Engineering, Institute of Aerodynamics and Gasdynamics, University of Stuttgart (2004).

[Mus96] A. Muschinsky, *A similarity theory of locally homogeneous and isotropic turbulence generated by a Smagorinsky-type LES*, JFM 325 (1996), 239-260.

[PB02] U. Piomelli and E. Balaras, *Wall-layer models for large eddy simulations*, Annual review of fluid mechanics 34 (2002), 349-374.

[Pope00] S. Pope, *Turbulent Flows,* Cambridge Univ. Press, 2000.

[Pru89] C. D. Pruett, *A fast algorithm for simulation of a spatially-evolving, two-dimensional, planar mixing layer*, Int. J. Num. Meth. Fluids, 76 (1989), p. 275.

[Pru00] C. D. Pruett, *On Eulerian time-domain filtering for spatial large-eddy simulation*, AIAA J., 38 (2000), p. 1634.

[Pru08] C. D. Pruett, *Temporal large-eddy simulation: theory and implementation*, Theor. Com-

put. Fluid Dyn. 22 (2008), pp. 275-304

[PGGT03] C. D. Pruett, T. B. Gatski, C. E. Grosch, and W. D. Thacker, *The temporally filtered Navier-Stokes equations: properties of the residual stress*, Phys. Fluids, 15 (2003), pp. 2127-2140.

[PTGG06] C. D. Pruett, B. C. Thomas, C. E. Grosch, and T. B. Gatski, *A temporal approximate deconvolution model for large-eddy simulation*, Phys. Fluids, 18 (2006), pp. 1-4.

[Re95] O. Reynolds, *On the dynamic theory of incompressible viscous fluids and the determination of the criterium*, Phil. Trans. R. Soc. London A 186(1895), 123-164.

[Ros89] Ph. Rosenau, *Extending hydrodynamics via the regularization of the Chapman-Enskog expansion*, Phys. Rev.A 40 (1989), 7193.

[Sag01] P. Sagaut,*Large eddy simulation for Incompressible flows,* Springer, Berlin, 2001.

[ST92] S. Schochet and E. Tadmor, *The regularized Chapman-Enskog expansion for scalar conservation laws*, Arch. Rat. Mech. Anal. 119 (1992), 95.

[SA99] S. Stolz and N. A. Adams, *An approximate deconvolution procedure for large eddy simulation*, Phys. Fluids, II(1999),1699-1701.

[SAK01a] S. Stolz, N. A. Adams and L. Kleiser, *The approximate deconvolution model for LES of compressible flows and its application to shock-turbulent-boundary-layer interaction*, Phys. Fluids 13 (2001),2985.

[SAK01b] S. Stolz, N. A. Adams and L. Kleiser, *An approximate deconvolution model for large eddy simulation with application to wall-bounded flows*, Phys. Fluids 13 (2001), 997.

[SAK02] S. Stolz, N. A. Adams and L. Kleiser, *The approximate deconvolution model for compressible flows: isotropic turbulence and shock-boundary-layer interaction*, in: Advances in LES of complex flows (editors: R. Friedrich and W. Rodi) Kluwer, Dordrecht, 2002.

[Tad93] E. Tadmor, *Total variation and error estimates for spectral viscosity approximations*, Mathematics of Computation 60 (1993) 245-256.